

Article

Using a Simple Magnetic Adsorbent for the Preconcentration and Determination of Ga(III) and In(III) by Electrothermal Atomic Absorption Spectrometry

Yesica Vicente-Martínez , María José Muñoz-Sandoval, Manuel Hernández-Córdoba  and Ignacio López-García * 

Department of Analytical Chemistry, Faculty of Chemistry, Regional Campus of International Excellence "Campus Mare Nostrum", University of Murcia, 30100 Murcia, Spain
* Correspondence: ilgarcia@um.es

Abstract: A solid-phase dispersive microextraction procedure has been developed using ferrite (Fe_3O_4), an inexpensive magnetic material, as an adsorbent for the separation and subsequent determination of Ga(III) and In(III). The ions were removed from an aqueous solution by adsorption on Fe_3O_4 , which was next easily collected from the medium by the action of a magnet. The analytes were then desorbed using 50 μL of 2 M NaOH or 50 μL of a 4:1 mixture of 0.1 M EDTA and 2 M HNO_3 for the determination of Ga(III) or In(III), respectively. The level of the elements in the desorption phase was measured by electrothermal atomic absorption spectrometry (ETAAS) by injecting 10 μL of this phase into the atomizer. The enrichment factor was 163, and detection limits of 0.02 and 0.01 $\mu\text{g L}^{-1}$ were achieved for Ga(III) and In(III), respectively. The reliability of the procedure has been verified by means of standard reference materials and by means of standard additions. Results are given for waters, soils and samples obtained from various electronic devices. It is of note that the procedure could be the basis for a useful way of recovering these valuable elements from different matrices for reuse.

Keywords: gallium; indium; adsorption; magnetic dispersive solid-phase microextraction; electrothermal atomic absorption spectrometry



Citation: Vicente-Martínez, Y.; Muñoz-Sandoval, M.J.; Hernández-Córdoba, M.; López-García, I. Using a Simple Magnetic Adsorbent for the Preconcentration and Determination of Ga(III) and In(III) by Electrothermal Atomic Absorption Spectrometry. *Molecules* **2023**, *28*, 2549. <https://doi.org/10.3390/molecules28062549>

Academic Editors: Victoria Samanidou and Irene Panderi

Received: 21 February 2023

Revised: 7 March 2023

Accepted: 8 March 2023

Published: 10 March 2023



Copyright: © 2023 by the authors. Licensee MDPI, Basel, Switzerland. This article is an open access article distributed under the terms and conditions of the Creative Commons Attribution (CC BY) license (<https://creativecommons.org/licenses/by/4.0/>).

1. Introduction

Semiconductor manufacturing has become an important industry in some developing countries. Gallium and indium are elements widely used in the manufacture of integrated circuits, liquid crystal displays (LCDs), light emitting diodes (LEDs) for backlighting and lighting, and various semiconductors [1,2]. These metals are released into the environment during processes such as etching, wet polishing and cleaning or e-waste recovery operations, which can generate many potentially hazardous waste products [3,4]. Accidental industrial spills can result in high concentrations of Ga and In oxides and arsenides in water, which have acute and chronic toxic effects on aquatic organisms.

On the other hand, since demand for them is very high, the need to recover these elements from manufactured products at the end of their useful life is becoming more and more evident. In this sense, some processes have recently been proposed for the recovery of indium by pre-leaching in $\text{HNO}_3 + \text{HF}$ using a new adsorbent material consisting of mesoporous activated carbon [5] or an electrode with titanium dioxide and activated carbon [6]. In both cases, the recovery is close to 85%. The use of a pulsed laser has been proposed for the release of indium oxide from semi-conductors [7] to avoid lengthy multi-stage removal processes. In the case of gallium recovery, even the most recently proposed processes do not achieve a quantitative recovery. Thus, algae-based sorbents [8], biogenic elemental tellurium nanoparticles [9], synthetic zinc refinery residues [10] and H-clinoptilolite [11] have been successfully used as adsorbents. The reported removal

efficiencies were, on average, 80% at low gallium concentrations (60% and 85% at 35 °C and 69 °C, respectively).

Whether or not recovery operations are carried out on these species, their presence in liquid effluents and wastes from production plants is increasing. Although these elements were initially thought to have little biological function and were not harmful to the human body, it has recently been reported that they can cause damage to human health [3]. In this regard, the Japanese Society for Occupational Health prescribed in 2007 that the maximum tolerable concentration of indium in serum should not exceed $3 \mu\text{g L}^{-1}$ [12]. In air, the German Ordinance on Hazardous Substances [13] sets a maximum permissible concentration of indium compounds at $0.1 \mu\text{g m}^{-3}$. As these elements accumulate in ecosystems, their toxic effects can be observed at the molecular, cellular and histological levels, even affecting the homeostasis of organisms [14]. Indium has no known biological function in living organisms [15]. The International Agency for Research on Cancer (IARC) classifies indium compounds in Group 2A, probably carcinogenic to humans [16]. Thus, indium contamination in the environment may pose a potential risk to public health via the food chain. On the other hand, the number of studies on the toxicity of Ga has been increasing until recently, and most of them support the conclusion that Ga has a very low toxicity [17], although this is highly dependent on the gallium compound and its way of entering the body [18].

The levels of these elements in soils vary considerably. The concentration of Ga in soils is usually between 3 and 70 mg kg^{-1} . The total average content of In in unpolluted soils is between 0.01 and 0.5 mg kg^{-1} . The distribution of In and Ga in soils mainly indicates their association with the clay fraction. In water samples, Ga and In concentrations are very low. The average concentration of Ga in seawater is 30 ng L^{-1} ; in rivers, it ranges globally from 1 to 22 ng L^{-1} . In the oceans, the concentration of In has been estimated to be about 0.1 ng L^{-1} [19]. In most environmental samples, the concentration of these elements is close to the detection limits of analytical techniques, hence the interest in having sensitive and selective methods for their determination.

Ga(III) can be determined by molecular absorption spectrometry using ligands that form compounds with high molar absorptivity [20–23], whose sensitivity can be improved by coupling to a liquid- [24] or solid-phase extraction procedure [25]. If the compound resulting from the interaction of Ga(III) with the ligand emits fluorescence, sensitivity is further enhanced [26]. When combined with solid-phase extraction, a limit of detection (LOD) of $3.1 \mu\text{g L}^{-1}$ can be achieved with Vis-UV detection [25].

However, atomic methods have undoubtedly been the most widely used for the determination of Ga(III). In the case of atomic absorption, flame atomization (FAAS) [27,28] and electrothermal [29–31] techniques (ETAAS) have been proposed, although the narrow linearity range characteristic of this technique has led many authors to use atomic emission spectrometry with optical detection (ICP-OES) [32–35] or mass spectrometry (ICP-MS) [36,37] for the purpose. These latter techniques are expensive, mainly due to the high argon consumption. This fact, together with interferences caused by overlapping spectral lines in ICP-OES or the high salt content of some samples, which is incompatible with ICP-MS, has led several authors to propose electrochemical methods, mainly based on anodic stripping voltammetry, that achieve similar detection limits [38–42].

Most of the recently proposed methods using atomic detection techniques couple preconcentration processes in different media. For example, supercritical fluid extraction [31], silica nanoparticles packed in a microcolumn [43], solid-phase extraction with a cation exchanger [34], non-ionic [25,44] or chelating [45], modified resins [46], halloysite nanotubes [30], silica gel modified with gallic acid [47] or simply extraction with organic solvents [28], at cloud point [27] and in ionic liquids [48].

In the case of In(III), analytical methods for trace determination include ETAAS [30,45,49–54], FAAS [27,55,56], ICP-OES [57–60] and ICP-MS [61–63]. To a lesser extent, because they do not achieve sufficient sensitivity, Vis-UV molecular absorption spectrometry [46,47,64–68] and electrochemical methods are used [40,41]. Preconcentration techniques are used when-

ever low detection limits are required to avoid interferences. Few microextraction techniques have been proposed for the determination of indium. Most of them use liquid–liquid dispersive microextraction [65,67], floating drop extraction [69], ultrasound-assisted extraction [70] or cloud point extraction [27,71]. Solid-phase extraction, in its different variants, has received more attention. Silica gel [49], chelating resins with suitable ligands [45,46,52,54,59], coprecipitation with chitosan [53] and sodium dodecyl sulphate modified activated carbon [50] have been proposed.

In recent years, dispersive micro-solid-phase extraction (DMSPE) has gained prominence due to its sensitivity and speed. In DMSPE, a small amount of sorbent is dispersed in the solution to induce an immediate interaction between the metal ions and the nanomaterial. In this sense, the use of halloysite nanotubes [30] for Ga(III) and In(III) separation and graphitic carbon nitride [60], oleic acid coated magnetic particles [56] and bentonite clay [72] for In(III) determination have been proposed.

In this work, the interaction of indium and gallium with ferrite, an easily synthesized and cheap magnetic material, has been studied. Although several processes using solid particles as adsorbent material in microextraction processes have been proposed, none is as easy to synthesize as the one proposed in this work, with the added advantage of easy separation of the adsorbent material using a magnetic field. After the adsorption on ferrite, the ions were desorbed in a different medium and submitted to ETAAS. The results obtained with this study show that, on the one hand, it was possible to quantify both species at trace concentrations, achieving high enrichment factors and low LODs for both species. On the other hand, the study of the adsorption of the species on ferrite is a simple and economical proposal for the recovery of these valuable species.

2. Results and Discussion

2.1. Effect of pH

The effect of pH on the retention of Ga(III) and In(III) ions by ferrite was studied in the range 3–10 by using different buffer solutions, and the results are shown in Figure 1. As can be seen from curve a, corresponding to Ga(III), the retention was practically total over the whole range studied, whereas the retention of In(III) reached a maximum in the range $7.5 < \text{pH} < 8.5$. In order to standardize the experimental procedure, the use of pH = 8 is recommended. The surface charge of the ferrite starts to become positive below pH = 6.5 (Figure S1). Therefore, at the pH found to be optimal for the retention of In(III) and Ga(III), the surface charge of the adsorbent material is negative.

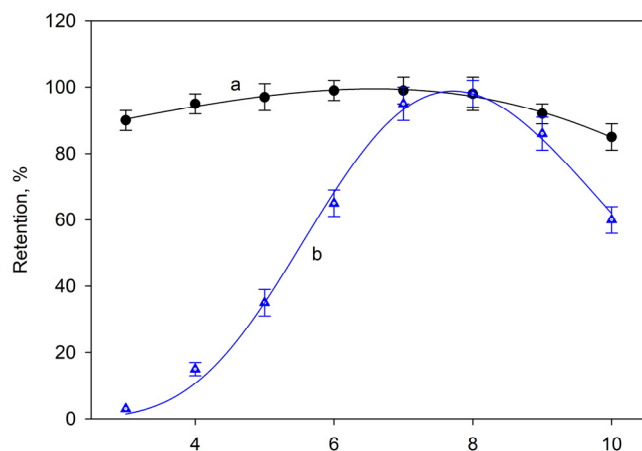


Figure 1. Effect of pH on Ga(III) and In(III) retention (curves a and b, respectively). Error bars correspond to the standard deviation of three determinations.

In the case of gallium, the existence of polynuclear species as opposed to mononuclear species has been described. Indeed, gallium(III) ions give rise to monomeric Ga(OH)_3 and Ga(OH)_4^- hydroxides together with polynuclear hydroxides such as $\text{Ga}_3(\text{OH})_{11}^{2-}$,

$\text{Ga}_4(\text{OH})_{11}^+$ and $\text{Ga}_6(\text{OH})_{15}^{3+}$ [73,74]. The tendency of Ga(III) to form polyionic hydroxides and the difficulty in determining mononuclear species seems to have been demonstrated. Indeed, the presence of $\text{Ga}_6(\text{OH})_{15}^{3+}$ formed around pH = 2.8 has been described. Figure S2 shows the gallium distribution taking into account these hydrolysis phenomena. These polynuclear hydroxides, together with $\text{Ga}(\text{OH})_3$, have been termed colloidal solid gallium [73,75,76]. Since the predominant species in the pH range studied is $\text{Ga}(\text{OH})_3$, we assume that this must be the species retained on the surface, although we must also consider the possible adsorption of gallium in the form of positively charged polynuclear hydroxylated complexes. Although as the degree of polymerization increases, the polyhydroxylated gallium complexes reduce their positive charge by converting the OH^- bridges into O^{2-} bridges, their ability to interact with anionic surfaces is clear and this would justify their adsorption on ferrite at pH values above 7.

In the case of In(III), the distribution of species at different pH values (Figure S3) indicates that the predominant species in the pH range studied is $\text{In}(\text{OH})_3$. However, the presence of chlorohydroxo complexes, mainly $\text{In}(\text{OH})\text{Cl}^+$ and to a lesser extent $\text{In}_2(\text{OH})\text{Cl}_4^+$, cannot be excluded. It is therefore assumed that it is the neutral $\text{In}(\text{OH})_3$ species which adsorb on the ferrite surface.

2.2. Effect of the Adsorbent Amount and the Time of Contact

The amount of ferrite required to achieve a quantitative retention of the analytes was studied. For this study, concentrations as high as $200 \mu\text{g L}^{-1}$ were used since they ensure that the results obtained will also be adequate for solutions with much lower concentrations and, at the same time, guarantee that even if some active sites are occupied by other species, there will still be enough available for the analytes.

The amount of adsorbent material was varied between 0 and $5 \mu\text{g}$, corresponding to suspension volumes of up to $300 \mu\text{L}$. Figure 2A shows the results obtained for the retention of Ga(III), those of In(III) being very similar. As shown in the graph, the retention becomes maximum and constant from about $1 \mu\text{g}$ of adsorbent. We conclude that the presence of only $1.7 \mu\text{g}$ of adsorbent material is sufficient to retain the tested concentrations of these ions. It can be predicted that at much lower analyte concentrations, as would be the case if the proposed preconcentration procedure is applied, the number of active sites for adsorption is guaranteed. It is therefore recommended that $100 \mu\text{L}$ of the adsorbent suspension is used for a 10 mL sample containing the analytes of interest.

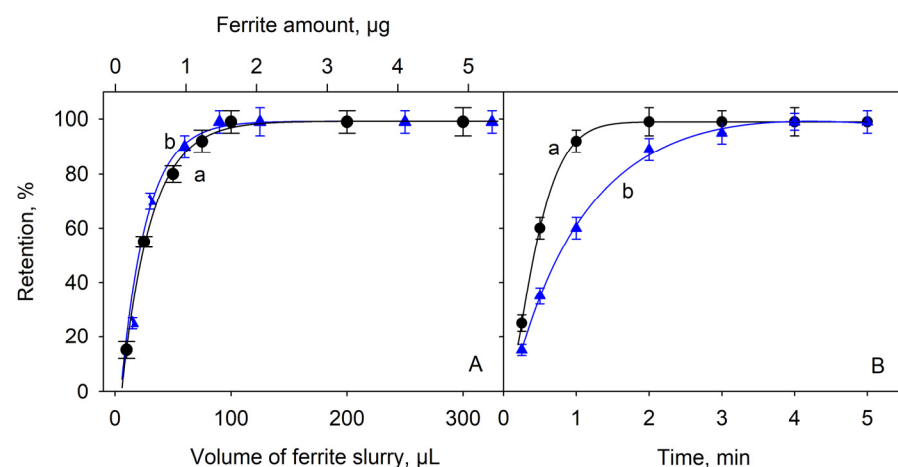


Figure 2. (A) Effect of contact time between Ga(III) and In(III) solutions (curves a and b, respectively) and adsorbent material on retention efficiency; (B) effect of the amount of adsorbent on the retention of Ga(III) and In(III) (curves a and b, respectively).

On the other hand, the contact time between the adsorbent and the solution containing the analytes was also studied. Figure 2B shows the influence of the contact time between these solutions and the adsorbent material when working at pH = 8 and room temperature.

The time was counted from the moment the ferrite was added until the neodymium magnet was applied to separate the solid phase. As can be seen, the retention increased rapidly during the first 2 min and it was complete in less than 4 min. This rapid increase in adsorption efficiency can be attributed to the large amount of vacant active sites on the adsorbent surface. When working with much lower concentrations of these ions to achieve a preconcentration effect, the time required will be much shorter, as already described for similar processes [77,78]. The results obtained for the retention of In(III) under the recommended experimental conditions were similar to those obtained for Ga(III). Therefore, a contact time of 5 min was adopted as sufficient to ensure quantitative retention of both species. Up to 25 mL of sample can be treated with 200 μ L of ferrite suspension and complete adsorption can be achieved in less than 10 min without changing the volume of desorption medium.

2.3. Study of the Desorption Conditions

The desorption of the analytes in a microvolume of liquid phase compatible with the detector is one of the main objectives to be achieved in a microextraction process. In this respect, the behavior of Ga(III) was very different from that of In(III). Figure 3 shows the desorption rates obtained for Ga(III) in different media. In all cases, 100 μ L was used as the desorption volume. As can be seen, all media were basic, as desorption in acidic media was very low. Each medium was tested with and without the use of ultrasound and at two temperatures: room temperature and 80 °C. Desorption was tested in: (a) 0.2 M NaOH; (b) 0.2 M NH₄OH; (c) 0.1 M tetramethylammonium hydroxide and (d) 0.1 M ethylenediaminetetraacetic acid disodium salt (EDTA) at pH = 12. The best results were obtained using 0.2 M sodium hydroxide and heating at 80 °C for 5 min in an ultrasonic bath. Under these conditions the desorption was quantitative.

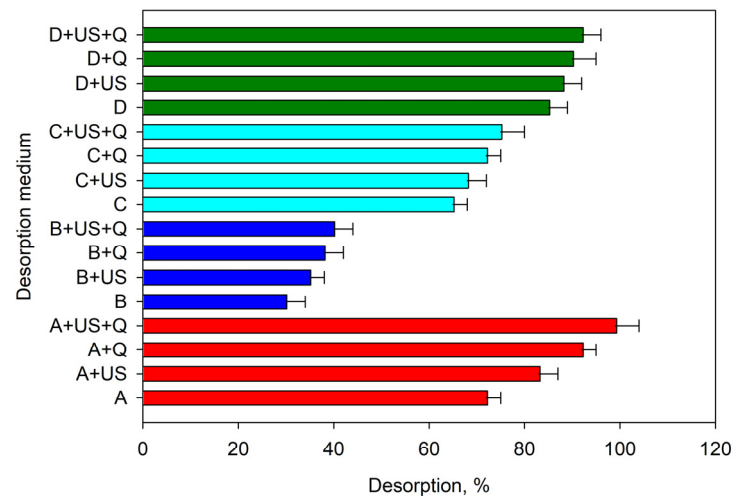


Figure 3. Effect of the desorption medium on the releasing of Ga(III) from the adsorbent to the aqueous phase. Media A (red), B (dark blue), C (blue) and D (green) correspond to 0.2 M NaOH, 0.2 M NH₄OH, 0.1 M TMHA and 0.1 M EDTA solutions, respectively. The terms US and Q correspond to the use of an ultrasonic bath for 5 min and heating at 80 °C, respectively.

For In(III), different media were tested at two temperatures (room temperature and 80 °C) and in the presence or absence of ultrasound. The media used were: (a) 0.2 M sodium hydroxide; (b) 0.005% *m/v* dithizone; (c) 0.05% *m/v* dithizone; (d) 0.01 M phenanthroline; (e) mixture of HF and HNO₃ acids at 8% in HF and 4% in HNO₃; (f) 0.1 M EDTA and (g) a medium consisting of 80 μ L of 0.1 M EDTA and 20 μ L of 2 M HNO₃. As shown in Figure 4, the best results were obtained using EDTA in acidic medium. Quantitative desorption was achieved by using 80 μ L of 0.1 M EDTA and 20 μ L of 2 M HNO₃ as desorption media and applying ultrasound for 2 min.

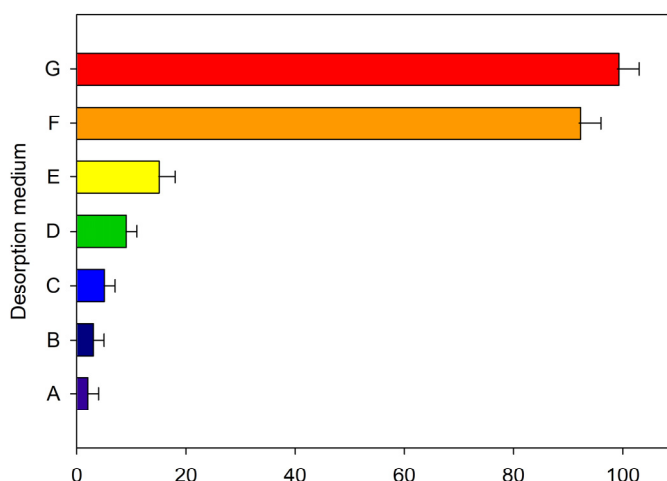


Figure 4. Effect of the desorption medium on the releasing of In(III) from the adsorbent to the aqueous phase. Media A–G correspond to 0.2 M NaOH, 0.005% *m/v* dithizone, 0.05% *m/v* dithizone, 0.01 M phenanthroline, HF + HNO₃; 0.1 M EDTA and a medium consisting of 80 μ L of 0.1 M EDTA and 20 μ L of 2 M HNO₃.

On the other hand, different volumes of desorption phase were assayed. As could be expected, as the desorption volume increased, and the analyte concentration, and thus the analytical signal, decreased. Finally, looking for a compromise between maximum (total) desorption and minimum dilution of the analytes, 50 μ L was selected as the volume to be used for desorption.

2.4. Optimization of the ETAAS Parameters

The resonance line suggested in the software of the spectrometer for the determination of gallium is 287.424 nm. However, this wavelength is not suitable for the purpose since iron presents an absorption line at 284.417 nm. Despite this line having a low sensitivity, it affects the analytical signal (see Figure 5A) due to the relatively large amount of iron involved. To avoid the deleterious effect, a secondary line of gallium, namely 294.346 nm, is recommended here. Using this line, no interference effect was observed and the selectivity was excellent (Figure 5B).

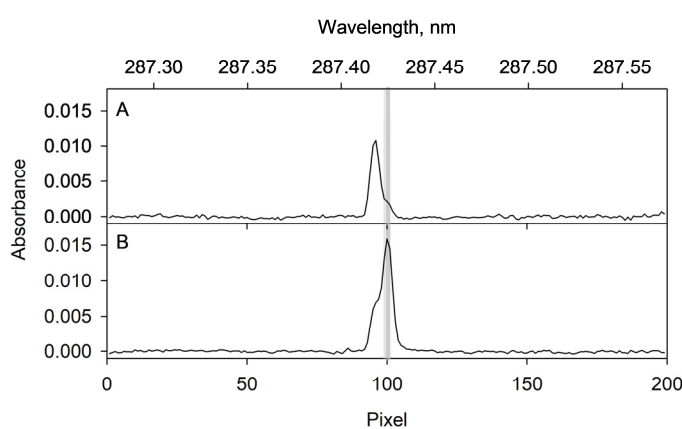


Figure 5. Average absorbance measured during the integration time at each observation pixel for the Ga wavelength at 287.424 nm. (A) corresponds to the signal from the desorption supernatant of a blank assay. (B) corresponds to the signal obtained for the desorption supernatant resulting from the application of the proposed procedure to a 2 μ g L⁻¹ Ga(III) solution. As can be seen, the absorption bands of Fe(III) and Ga(III) overlap. The grey band corresponds to pixels 99, 100 and 101, from which the analytical signal is calculated.

In the case of indium determination, the resonance wavelength of 303.935 nm was chosen since the signal obtained at this wavelength is not affected by the presence of iron (Figure 6).

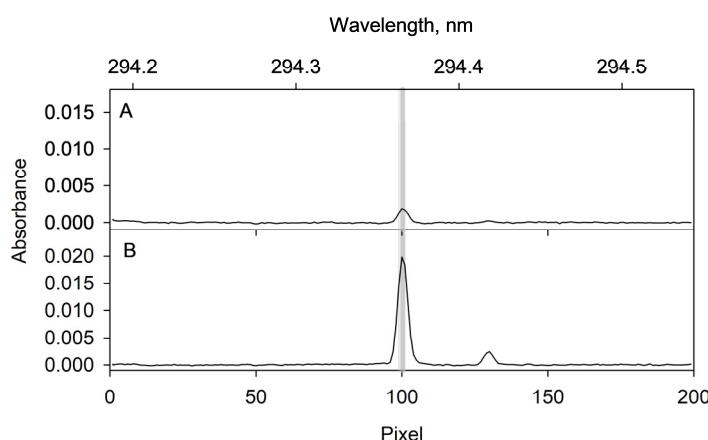


Figure 6. Absorbance averaged over the integration time at each observation pixel for the Ga measurement at 294.364 nm. (A) corresponds to the signal from the desorption supernatant of a blank assay. (B) corresponds to the signal obtained for the desorption supernatant when the proposed procedure is applied to a $2 \mu\text{g L}^{-1}$ Ga(III) solution. The grey band corresponds to pixels 99, 100 and 101 from which the analytical signal is calculated. The small absorption band due to gallium at 294.417 nm is also visible.

The convenience of using a chemical modifier for the atomization stage was also considered [79]. The results showed that for the determination of gallium, the use of palladium nitrate as a chemical modifier was suitable to improve sensitivity and to obtain signals with low background absorption.

Similar studies were carried out for the indium determination, testing different common chemical modifiers, and again palladium proved suitable. Therefore, the procedure includes the injection into the atomizer of $10 \mu\text{L}$ of a 500 mg L^{-1} Pd(II) solution as a chemical modifier.

The calcination and atomization temperatures were optimized in the usual way, looking for low background and well-defined atomization profiles, and the results are included in Table 1 where the rest of parameters are summarized.

Table 1. Instrumental parameters and heating program for Ga and In.

Parameter			
Wavelength, nm	294.364 (Ga)/303.935 (In)		
Slit, nm	0.7		
Atomizer	Transversal with L'Vov platform		
Background correction	Zeeman effect		
Injected sample volume, μL	10		
Chemical modifier	10 μL of 500 mg L^{-1} Pd(II) solution		
Sample volume, mL	10		
Heating program			
Step	Temperature, $^{\circ}\text{C}$	Ramp, $^{\circ}\text{C s}^{-1}$	Hold, s
1: Dry	110	10	20
2: Dry	130	9	10
3: Calcination	1300	300	15
4: Atomization ^{a,b}	2300 (Ga)/2200 (In)	2300 (Ga)/1500 (In)	5
5: Clean	2450	500	4

^a Internal argon flow stopped 5 s before. ^b Reading step.

2.5. Analytical Figures of Merit: Applications

Using the conditions optimized, a linear behavior was found between the peak area signal and the concentration of gallium or indium species in solution in the range 0.1–1.5 and 0.05–1 $\mu\text{g L}^{-1}$, respectively. The slopes of the calibration lines were 0.414 ± 0.005 and $0.683 \pm 0.007 \text{ s } \mu\text{g}^{-1} \text{ L}$, and the limits of detection, calculated from the threefold standard error of the regression, were 0.02 and 0.01 $\mu\text{g L}^{-1}$ for gallium and indium, respectively. The relative standard deviation of the measurements within the calibration range was between 4.2 and 4.8%.

The enrichment factor was calculated from the ratio between the slopes measured after application of the microextraction procedure and those obtained directly, and was found to be 163 ± 2 when the volume of aqueous phase was 10 mL and a volume of 50 μL of the corresponding solvent was used for desorption.

Table 2 shows the main procedures reported in the recent literature for the determination of both analytes and involving liquid–liquid or liquid–solid microextraction processes for preconcentration. As can be seen, the procedure studied in this work successfully competes with those already reported since it allows a high preconcentration factor to be achieved with minimal sample consumption, furthermore involving an affordable and selective technique for quantification.

Table 2. Characteristics of some procedures reported for the determination of Ga and In with the use of microextraction techniques.

Analyte	Separation Technique	TD	V	FE	LOD	Ref.
Ga, In	SPE with aminated silica gel functionalized with HBAAS	FAAS	1000	200	4.1; 1.55	[80]
Ga, In	SPE with aminated silica gel functionalized with gallic acid	FAAS	50	250	5.8; 1.8	[47]
In	SPE with TiO_2	Vis-UV	25	25	450	[68]
In	SPE with Chromosorb 108 and bathocuproine disulphonic acid	ETAAS	100	30	0.012	[54]
In	SPE with SDS-modified activated carbon	ETAAS	200	363	0.0002	[50]
In	DMSPE with exfoliated graphitic carbon nitride nanosheets	ICP-OES	10	75	0.32	[60]
Ga, In	USA-DMSPE with halloysite nanotubes	ETAAS	10	33; 37	0.02; 0.01	[30]
In	VASPME with oleic acid coated ferrite	FAAS	30	44	6.02	[56]
In	DLSME with chitosan	ETAAS	500	100	0.4	[53]
Ga	CPE with 8-hydroxyquinoline and Triton X-114	ICP-MS	50	20	1.2	[71]
Ga, In	CPE with gallic acid on Triton X-114	FAAS	25	54; 48	3.5; 1.25	[27]
Ga, In	CPE with 5-Br-PADAP in the presence of Triton X-100	ICP-OES	25	12	0.7; 0.3	[81]
Ga	DLLME with APDC	XRF	5	250	1.7	[82]
In	DLLME with PAN	Vis-UV	10	160	0.3	[65]
Ga	USA-DLLME with PAN in chlorobenzene	FAAS	40	124	70	[70]
In	SFOD-DLLME with dithizone and 1-undecanol	Vis-UV	10	36	9	[67]
In	SFOD-DLLME with PAN and 1-undecanol	ETAAS	25	62,5	0.05	[69]
Ga, In	MDSPE with ferrite	ETAAS	10	163	0.02; 0.01	TW

TD: detection technique; V: sample volume, mL; FE: enrichment factor; LOD: limit of detection, $\mu\text{g L}^{-1}$; Ref: reference; TW: this work; SPE: solid-phase extraction; HBAAS: 2-hydroxy-5-(2-hydroxybenzylideneamino)benzoic acid; CPE: cloud point extraction; 5-Br-PADAP: 2-(5-bromo-2-pyridinazo)-5-diethylaminophenol; SDS: sodium dodecyl sulphate; DMSPE: dispersive micro-solid-phase extraction; USA-DMSPE: ultrasonic-assisted dispersive micro-solid-phase extraction; VASPME: vortex-assisted solid-phase microextraction; DLSME: dispersive liquid–solid microextraction; XRF: X-ray fluorescence; PAN: 1-(2-pyridinazo)-2-naphthol; USA-DLLME: ultrasonic-assisted liquid–liquid dispersive microextraction; SFOD-DLLME: floating solid droplet DLLME; MDSPE: magnetic dispersive solid-phase microextraction.

To test its usefulness and reliability, the procedure studied was applied to the determination of gallium and indium ions in four water samples (tap water, sea water and two bottled water samples). The reliability was first assessed by applying the standard additions method and, as shown in Table 3, the recoveries of the spiked samples were satisfactory at the 95% confidence level.

Table 3. Results of Ga(III) and In(III) in real water samples (RWS).

RWS	Ga(III), $\mu\text{g L}^{-1}$			In(III), $\mu\text{g L}^{-1}$		
	Added	Found ^a	Rec., %	Added	Found ^a	Rec., %
M1	0	<LOD	-	0	<LOD	-
	0.2	0.19 \pm 0.02	95 \pm 6	0.1	0.10 \pm 0.02	103 \pm 6
M2	0.4	0.42 \pm 0.02	105 \pm 7	0.3	0.29 \pm 0.02	98 \pm 7
	0	<LOD	-	0	<LOD	-
M3	0.2	0.21 \pm 0.03	105 \pm 6	0.1	0.09 \pm 0.02	92 \pm 5
	0.4	0.38 \pm 0.02	95 \pm 5	0.3	0.31 \pm 0.03	104 \pm 5
M4	0	<LOD	-	0	<LOD	-
	0.2	0.21 \pm 0.02	105 \pm 5	0.1	0.11 \pm 0.02	110 \pm 6
	0.4	0.39 \pm 0.03	98 \pm 6	0.3	0.32 \pm 0.03	107 \pm 7
	0	<LOD	-	0	<LOD	-
	0.2	0.18 \pm 0.03	90 \pm 6	0.1	0.09 \pm 0.02	93 \pm 6
	0.4	0.41 \pm 0.03	103 \pm 4	0.3	0.31 \pm 0.04	103 \pm 5

M1: drinking water from the supply network; M2: sea water; M3 and M4: bottled water. ^a mean value \pm standard deviation of three determinations.

The reliability was further confirmed by measuring the gallium and indium content in several standard reference materials (SRMs): NIST SRM 2711, NCS DC 73319a, TM-25.4 and TMDA-62.2. As two of them did not contain indium, they were analyzed before and after their fortification with indium ($0.5 \mu\text{g L}^{-1}$) and relative recoveries of 93 to 107% and RSDs of 7 to 9% were obtained. The analytical data obtained are summarized in Table 4. These results demonstrate that the proposed method, together with the instrumentation used, is suitable for the analysis of soil, sediment and water samples.

Table 4. Results of Ga(III) and In(III) in reference materials.

SRM	Ga(III), $\mu\text{g g}^{-1}$		In(III), $\mu\text{g g}^{-1}$	
	Certificate	Found ^a	Certificate	Found
NIST SRM 2711 ^b (soil)	15	15.8 \pm 0.4	1.1	1.2 \pm 0.1
NCS DC 73319a (soil)	18 \pm 1.4	17.9 \pm 0.3	0.12 \pm 0.02	0.12 \pm 0.01
Ga(III), $\mu\text{g L}^{-1}$		In(III), $\mu\text{g L}^{-1}$		
SRM	Certificate	Found	Certificate	Found
TM-25.4 (water)	32.6 \pm 2.8	33.2 \pm 0.5	-	<LOD
TMDA-62.2 (water)	9.03 \pm 0.73	8.98 \pm 0.23	-	<LOD

^a mean value \pm standard deviation of three determinations. ^b noncertified values.

The procedure studied was also applied to the determination of gallium and indium in various electronic devices, namely three mobile phones of very different dates of manufacture, the screens of two non-touch laptop computers and the diodes of several LED light bulbs. All these devices were treated according to the procedure described in Section 3.3. The levels of the two elements found are shown in Table 5. For LCD panels, the values shown correspond to the contents in the panels after removal of the polymer frames protecting the LCD structure (which were not attached to the LCD panel). The polymeric polarizing film, which remained strongly adhered to the glass surface, was then removed in an acetone bath. This made it easier to grind the material.

Table 5. Determination of gallium and indium in optoelectronic devices.

Sample Treatment		Ga(III), $\mu\text{g g}^{-1}$			In(III), $\mu\text{g g}^{-1}$		
Calcination	Added	Found ^a	Rec., %	Added	Found ^a	Rec., %	
LED light bulb	-	730 ± 3	-	-	20 ± 2	-	
	20	749 ± 4	99.8 ± 3.7	20	41 ± 2	102.5 ± 4.7	
LCD Phone 1	-	5.1 ± 0.2	-	-	160 ± 4	-	
	20	25.3 ± 0.3	100.8 ± 3.7	20	178 ± 5	98.9 ± 2.8	
LCD Phone 2	-	287 ± 2	-	-	412 ± 6	-	
	20	306 ± 3	99.7 ± 3.7	20	434 ± 6	100.4 ± 1.4	
LCD Phone 3	-	190 ± 2	-	-	580 ± 6	-	
	20	212 ± 4	100.9 ± 3.7	20	596 ± 5	99.3 ± 0.9	
Laptop screen 1	-	215 ± 3	-	-	360 ± 5	-	
	20	236 ± 4	100.4 ± 3.7	20	378 ± 5	99.5 ± 1.3	
Laptop screen 2	-	410 ± 2	-	-	265 ± 4	-	
	20	432 ± 4	100.4 ± 3.7	20	283 ± 5	99.3 ± 1.7	
Leaching		Ga(III), $\mu\text{g g}^{-1}$			In(III), $\mu\text{g g}^{-1}$		
Leaching	Added	Found ^a	Rec., %	Added	Found ^a	Rec., %	
LED light bulb	-	730 ± 3	-	-	20 ± 2	-	
	20	749 ± 4	99.8 ± 0.5	20	41 ± 2	102.5 ± 4.9	
LCD phone 1	-	3.8 ± 0.2	-	-	112 ± 3	-	
	20	23.3 ± 0.3	97.9 ± 1.3	20	133 ± 4	100.7 ± 3.0	
LCD phone 2	-	280 ± 2	-	-	403 ± 6	-	
	20	302 ± 3	100.7 ± 0.9	20	424 ± 6	102.0 ± 1.4	
LCD phone 3	-	184 ± 2	-	-	551 ± 5	-	
	20	205 ± 4	100.5 ± 1.9	20	569 ± 5	99.6 ± 0.9	
Laptop screen 1	-	198 ± 4	-	-	327 ± 4	-	
	20	223 ± 5	102.3 ± 2.2	20	349 ± 5	100.6 ± 1.4	
Laptop screen 2	-	389 ± 4	-	-	252 ± 4	-	
	20	411 ± 4	100.5 ± 0.9	20	270 ± 5	99.2 ± 1.8	

^a mean value ± standard deviation of three determinations.

3. Materials and Methods

3.1. Materials and Instrumentation

All the solutions were prepared with deionized water (resistivity > 18 MΩ cm) purified using a Millipore system (Millipore, Bedford, MA, USA). Glassware was washed with 10% v/v nitric acid solution and rinsed with this pure water before use.

Ga(III) and In(III) standards were prepared from 1 g L⁻¹ standard solutions supplied by Panreac (Barcelona, Spain). FeCl₃·6H₂O, FeCl₂·4H₂O (Sigma, St. Louis, MO, USA) and ammonium hydroxide (Merck, Darmstadt, Germany) were used for the synthesis of the ferrite particles. A 10 g L⁻¹ solution of Pd(NO₃)₂ (Sigma-Aldrich) was used as a chemical modifier. The rest of the reagents were from Merck or Sigma-Aldrich.

All atomic absorption measurements were carried out with a high-resolution continuous-source atomic absorption spectrometer (HR-CS-AAS, model contrAA 700) provided by Analytik Jena AG (Jena, Germany) and equipped with a transversely heated graphite atomizer. The furnace heating program and the optimized experimental conditions are summarized in Table 1.

A 50 W ultrasonic bath model LT-80pro (Terratech, Barcelona, Spain) with temperature control was used for thermal and ultrasonic treatments. Vortexing was carried out with a Reax Top from Heidolph (Schwabach, Germany). For centrifugation, a Hettich Eba 200 centrifuge (Tuttlingen, Germany) with rotor and adapter for 15 mL conical bottom tubes at up to 6000 rpm was used. Samples, when necessary, were ground in an agate ball mill model MM2 from Retsch (Haan, Germany). Mineralization of the samples was carried out using an Anton Paar Multiwave 3000 microwave oven (Graz, Austria). For

calcination of the samples, when required, a Hobersal GB 7-122 muffle furnace (Barcelona, Spain) was used.

Magnetic discs (Supermagnete, Gottmadingen, Germany) were used for magnetic separation during the synthesis of the nanoparticles and their removal from the aqueous medium.

3.2. Preparation of the Magnetic Material

Fe_3O_4 particles were prepared by the coprecipitation procedure described in [83], with slight modifications. In this process, 20 mL water (from which the oxygen has been removed by a stream of nitrogen) was heated to 80 °C and then 0.56 g $\text{FeCl}_3 \cdot 6\text{H}_2\text{O}$ and 0.2 g $\text{FeCl}_2 \cdot 4\text{H}_2\text{O}$ were added while stirring continuously. After dissolution of the solids, 2 mL of concentrated ammonium hydroxide was added. The black precipitate that appeared was shaken at 80 °C for 1 h. The magnet was then applied so that the ferrite particles were attracted to the wall of the tube and the supernatant was removed by decantation. The Fe_3O_4 particles were then washed with 20 mL portions of water and decanted in the same way until the pH of the solution was neutral. Finally, the iron particles (about 0.34 g Fe_3O_4) were suspended in 20 mL of water and kept refrigerated for use.

Particle size and zeta potential data for the adsorbent materials were obtained, and the results are given as Supplementary Materials (Figures S4 and S1, respectively). Figure S5 shows the Field Effect Scanning Electron Microscopy (FESEM) image corresponding to the surface of Fe_3O_4 . In addition, Figure S6 shows the associated Energy Dispersive X-ray (EDX) spectra and the atomic concentration table for Fe_3O_4 . The former displays strong peak signals for Fe and O. Signals for Al, Cu, Si and C correspond to the sample holder and the grid employed to obtain the FESEM images.

3.3. Samples Treatment

Water samples were filtered through a 0.45 μm syringe filter and then stored in polyethylene bottles at 4 °C for a maximum of 7 days.

Soil samples were treated by microwave-assisted wet digestion. Approximately 500 mg of the powdered certified reference material was placed in the PTFE container of the microwave system and 1 mL of 30% H_2O_2 was added to wet the sample. Then, 4 mL of 65% HNO_3 and 2 mL of 40% HF were added. After digestion (180 °C for 20 min), the clear solutions were transferred to calibrated 10 mL flasks and diluted according to the concentration of the analytes.

Light emitting diodes and mobile phone and laptop screens were first manually disassembled and separated into the different fractions. The polarizing polymer film, which remained strongly adhered to the surface of the display glass, was removed using an acetone bath. The samples were then cut into small pieces (approximately 1 × 1 cm) and ground in a ball mill for 120 min. Finally, the LED powder obtained was sieved through a 100 μm sieve [84]. To determine the total Ga and In contents, the powder was mixed with Na_2CO_3 in a 1:1 ratio and calcined (800–1100 °C), the furnace temperature being increased linearly at 10 °C min^{-1} [85]. The ashes were dissolved with 0.5 M H_2SO_4 and appropriately diluted depending on the amounts of indium and gallium involved.

For the leachates, the soil samples were treated with 1 M H_2SO_4 using a liquid to solid ratio of 50:1 at 90 °C and mechanical stirring for 60 min [85].

3.4. Procedure for the Determination of Gallium and Indium

The sample or standard solution was adjusted to pH = 8 with HNaCO_3 and the addition of small volumes of 0.1 M HNO_3 or NaOH, if necessary. After 5 min manual shaking, 100 μL of the Fe_3O_4 suspension prepared as indicated above was added. The adsorbent phase was separated with the neodymium magnet and the supernatant was discarded. For the determination of gallium, 50 μL of 2 M NaOH was added to the solid phase and the mixture was vortexed for 30 s. It was then placed in an ultrasonic bath at 80 °C for 5 min, the magnet being applied again to separate the solid. Next, 10 μL aliquots

of the supernatant phase were taken and injected according to the heating program given in Table 1.

For the determination of indium, desorption from the adsorbent was carried out using a medium consisting of 80 μ L of 0.1 M EDTA and 20 μ L of 2 M HNO₃. After vortexing for 30 s and holding the mixture at 80 °C for 5 min, the magnet was reapplied and the supernatant (10 μ L) injected into the atomizer.

4. Conclusions

Electrothermal atomic absorption spectrometry in conjunction with a simple magnetic dispersive solid-phase microseparation step has proved suitable for the purpose of determining low concentrations of gallium and indium. The adsorbent used (Fe_3O_4) is cheap and easy to obtain and, due to its magnetic properties, can be conveniently removed from the medium by the action of a magnet, thus avoiding the need for a centrifugation step. It is interesting to note that, in addition to the sensitive and selective analytical procedures here studied, the characteristics of this simple magnetic material open the door to its use for the recuperation or removal of the gallium and indium present in some residues.

Supplementary Materials: The following supporting information can be downloaded at: <https://www.mdpi.com/article/10.3390/molecules28062549/s1>; Figure S1: Zeta potential of ferrite particles synthetized as indicated in Experimental measured with dynamic light scattering (DLS); Figure S2: Distribution diagram of the hydrolysed forms of Ga(III) considering the polynuclear species (adapted from [73]); Figure S3: Distribution diagram for hydrolysed forms of In(III) (adapted from [86]); Figure S4: Dynamic Light Scattering (DSL) particle size distribution analysis obtained from ferrite particles synthetized as indicated in the work; Figure S5: FESEM image for Fe_3O_4 and Figure S6: EDX spectra and atomic concentration tables corresponding to the area shows in Figure S5 for Fe_3O_4 .

Author Contributions: Conceptualization, I.L.-G.; methodology, I.L.-G. and M.J.M.-S.; investigation, M.J.M.-S. and Y.V.-M.; data curation, I.L.-G., M.J.M.-S. and M.H.-C.; writing—original draft preparation, Y.V.-M.; writing—review and editing, M.H.-C. and I.L.-G.; supervision, M.J.M.-S.; funding acquisition, M.H.-C. All authors have read and agreed to the published version of the manuscript.

Funding: The authors acknowledge the financial support of the Spanish MCIN (Project PID2021-123201NB-I00 financed by MCIN/AEI/10.13039/501100011033/FEDER, UE).

Institutional Review Board Statement: Not applicable.

Informed Consent Statement: Not applicable.

Data Availability Statement: Data are available from the corresponding authors upon reasonable request.

Acknowledgments: M.J.M.-S. acknowledges a fellowship from the University of Murcia.

Conflicts of Interest: The funders had no role in the design of the study; in the collection, analyses, or interpretation of data; in the writing of the manuscript; or in the decision to publish the results. The authors declare no conflict of interest.

Sample Availability: Samples of the compounds Laptop screen 1 and 2 are available from the authors.

References

- Petrov, A.G. Liquid crystal physics and the physics of living matter. *Mol. Cryst. Liq. Cryst.* **1999**, *332*, 577–584. [[CrossRef](#)]
- Liu, L.; Keoleian, G.A. LCA of rare earth and critical metal recovery and replacement decisions for commercial lighting waste management. *Resour. Conserv. Recycl.* **2020**, *159*, 104846. [[CrossRef](#)]
- Bomhard, E.M. The toxicology of indium oxide. *Environ. Toxicol. Pharmacol.* **2018**, *58*, 250–258. [[CrossRef](#)]
- Crichton, T. Electronic waste management. *Trans. IMF* **2020**, *98*, 62. [[CrossRef](#)]
- Díez, E.; Gómez, J.; Rodríguez, A.; Bernabé, I.; Sáez, P.; Galán, J. A new mesoporous activated carbon as potential adsorbent for effective indium removal from aqueous solutions. *Microporous Mesoporous Mater.* **2020**, *295*, 109984. [[CrossRef](#)]
- Yen, C.H.; Chuang, S.-H.; Huang, R.-Y.; Liu, P.-I.; Chang, M.-C.; Horng, R.-Y. Titanium Dioxide/Activated Carbon Electrode with Polyurethane Binder for the Removal of Indium Ions via Capacitive Deionization. *Processes* **2021**, *9*, 1427. [[CrossRef](#)]

7. Leong, C.Y.; Yap, S.S.; Ong, G.L.; Ong, T.S.; Chin, Y.T.; Lee, S.F.; Tou, T.Y.; Nee, C.H. Single pulse laser removal of indium tin oxide film on glass and polyethylene terephthalate by nanosecond and femtosecond laser. *Nanotechnol. Rev.* **2020**, *9*, 1539–1549. [[CrossRef](#)]
8. Li, M.; Shadman, F.; Ogden, K.L. Algae-based sorbents for removal of gallium from semiconductor manufacturing wastewater. *Clean Technol. Environ. Policy* **2018**, *20*, 899–907. [[CrossRef](#)]
9. Saikia, S.; Sinharoy, A.; Lens, P.N. Adsorptive removal of gallium from aqueous solution onto biogenic elemental tellurium nanoparticles. *Sep. Purif. Technol.* **2022**, *286*, 120462. [[CrossRef](#)]
10. Saikia, S.; Costa, R.B.; Sinharoy, A.; Cunha, M.P.; Zaiat, M.; Lens, P.N. Selective removal and recovery of gallium and germanium from synthetic zinc refinery residues using biosorption and bioprecipitation. *J. Environ. Manag.* **2022**, *317*, 115396. [[CrossRef](#)] [[PubMed](#)]
11. Saez, P.; Rodríguez, A.; Gómez, J.M.; Paramio, C.; Fraile, C.; Díez, E. H-Clinoptilolite as an Efficient and Low-Cost Adsorbent for Batch and Continuous Gallium Removal from Aqueous Solutions. *J. Sustain. Met.* **2021**, *7*, 1699–1716. [[CrossRef](#)]
12. Ding, C.G.; Wang, H.Q.; Song, H.B.; Li, Z.H.; Li, X.P.; Ye, S.S.; Zhang, F.G.; Cui, S.W.; Yan, H.F.; Li, T. Occupational Exposure to Indium of Indium Smelter Workers. *Biomed. Environ. Sci.* **2016**, *29*, 379–384. [[CrossRef](#)]
13. AGS. Begründung zu Indium, Indium Oxid, Indium Hydroxid, Indium Phosphid in TRGS 900. 2017. Available online: https://www.baua.de/DE/Angebote/Rechtstexte-und-Technische-Regeln/Regelwerk/TRGS/pdf/900/900-indium-und-verbindungen.pdf?__blob=publicationFile&v=2 (accessed on 7 March 2023).
14. Chitambar, C.R. Medical Applications and Toxicities of Gallium Compounds. *Int. J. Environ. Res. Public Health* **2010**, *7*, 2337–2361. [[CrossRef](#)]
15. Ladenberger, A.; Demetriadis, A.; Reimann, C.; Birke, M.; Sadeghi, M.; Uhlbäck, J.; Andersson, M.; Jonsson, E. GEMAS: Indium in agricultural and grazing land soil of Europe—Its source and geochemical distribution patterns. *J. Geochem. Explor.* **2015**, *154*, 61–80. [[CrossRef](#)]
16. Beyersmann, D.; Hartwig, A. Carcinogenic metal compounds: Recent insight into molecular and cellular mechanisms. *Arch. Toxicol.* **2008**, *82*, 493–512. [[CrossRef](#)]
17. Schen, S.; Zhao, R.; Sun, X.; Wang, H.; Li, L.; Liu, J. Toxicity and Biocompatibility of Liquid Metals. *Adv. Healthc. Mater.* **2022**, *12*, 2201924. [[CrossRef](#)]
18. Bomhard, E.M. The toxicology of gallium oxide in comparison with gallium arsenide and indium oxide. *Environ. Toxicol. Pharmacol.* **2020**, *80*, 103437. [[CrossRef](#)] [[PubMed](#)]
19. Kabata-Pendias, H.A.; Mukherjee, A.B. *Trace Elements from Soil to Human*; Springer: Berlin/Heidelberg, Germany, 2007.
20. Arain, G.; Devi, I.; Khuhawar, M.Y. Spectrophotometric determination of gallium(III) as bipyridylglyoxal bis(4-phenyl-3-thiosemicarbazone) derivative. *Asian J. Chem.* **2007**, *19*, 5169–5176.
21. Avan, A.A. Spectrophotometric and colorimetric determination of gallium (III) with p-aminohippuric acid-functionalized citrate capped gold nanoparticles. *Turk. J. Chem.* **2021**, *45*, 879–891. [[CrossRef](#)] [[PubMed](#)]
22. Połedniok, J. Speciation of scandium and gallium in soil. *Chemosphere* **2008**, *73*, 572–579. [[CrossRef](#)] [[PubMed](#)]
23. Racheva, P.; Stojnova, K.T.; Lekova, V.; Dimitrov, A.N. Spectrophotometric Determination of Gallium(III) with 4-(2-Pyridylazo)-resorcinol and Nitron. *Croat. Chem. Acta* **2015**, *88*, 159–163. [[CrossRef](#)]
24. Stojnova, K.T.; Divarov, V.V.; Racheva, P.; Lekova, V.D. Extraction-Spectrophotometric Method for Determination of Gallium(III) in the Form of Ion Associate with a Monotetrazolium Salt. *J. Appl. Spectrosc.* **2015**, *82*, 853–856. [[CrossRef](#)]
25. Amin, A.S.; Moalla, S.M.N. Utility of solid phase extraction for UV-visible spectrophotometric determination of gallium in environmental and biological samples. *RSC Adv.* **2015**, *6*, 1938–1944. [[CrossRef](#)]
26. Kara, D.; Fisher, A.; Foulkes, M.; Hill, S.J. Determination of gallium at trace levels using a spectrofluorimetric method in synthetic U–Ga and Ga–As solutions. *Spectrochim. Acta Part A Mol. Biomol. Spectrosc.* **2010**, *75*, 361–365. [[CrossRef](#)]
27. Mortada, W.I.; Kenawy, I.M.; Hassanien, M.M. A cloud point extraction procedure for gallium, indium and thallium determination in liquid crystal display and sediment samples. *Anal. Methods* **2015**, *7*, 2114–2120. [[CrossRef](#)]
28. Pashajanov, A.M.; Bayramov, S.M.; Abbasova, G.G.; Agamaliyeva, M.M.; Mamedova, Z.A. Extraction-Atomic-Absorption Determination of Gallium (III) with 2-hydroxy-5-T-butylphenol-4'-methoxy-azobenzene. *J. Mater. Sci. Chem. Eng.* **2020**, *8*, 24–30. [[CrossRef](#)]
29. Arslan, Z.; Tyson, J.F. Slurry sampling for determination of lead in marine plankton by electrothermal atomic absorption spectrometry. *Microchem. J.* **2007**, *86*, 227–234. [[CrossRef](#)]
30. Krawczyk-Coda, M. Sequential determination of gallium, indium, and thallium in environmental samples after preconcentration on halloysite nanotubes using ultrasound-assisted dispersive micro solid-phase extraction. *New J. Chem.* **2018**, *42*, 15444–15452. [[CrossRef](#)]
31. Wu, C.-C.; Liu, H.-M. Determination of gallium in human urine by supercritical carbon dioxide extraction and graphite furnace atomic absorption spectrometry. *J. Hazard. Mater.* **2009**, *163*, 1239–1245. [[CrossRef](#)]
32. Cheng, Y.; Peng, H.X. Determination of the Impurity Element Gallium in the Metallic Aluminum Products such as Aluminum and Aluminum Alloy by ICP-OES. *Adv. Mater. Res.* **2013**, *706–708*, 60–63. [[CrossRef](#)]
33. De Santana, F.A.; Barbosa, J.T.; Matos, G.D.; Korn, M.G.; Ferreira, S.L. Direct determination of gallium in bauxite employing ICP OES using the reference element technique for interference elimination. *Microchem. J.* **2013**, *110*, 198–201. [[CrossRef](#)]

34. Gong, Q.; Wei, X.; Wu, J.; Min, F.; Liu, Y.; Guan, Y. A solid phase extraction method for determination of trace gallium in aluminum–iron samples by atomic spectrometry. *J. Anal. At. Spectrom.* **2012**, *27*, 1920–1927. [[CrossRef](#)]
35. Li, H.; Zu, W.; Liu, F.; Wang, Y.; Yang, Y.; Yang, X.; Liu, C. Determination of gallium in water samples by atomic emission spectrometry based on solution cathode glow discharge. *Spectrochim. Acta Part B At. Spectrosc.* **2019**, *152*, 25–29. [[CrossRef](#)]
36. Blokhin, M.; Zarubina, N.V.; Mikhailyk, P.E. Inductively coupled plasma mass spectrometric measurement of gallium in ferromanganese crusts from the Sea of Japan. *J. Anal. Chem.* **2014**, *69*, 1237–1244. [[CrossRef](#)]
37. Filatova, D.G.; Seregina, I.F.; Foteva, L.S.; Pukhov, V.V.; Timerbaev, A.R.; Bolshov, M.A. Determination of gallium originated from a gallium-based anticancer drug in human urine using ICP-MS. *Anal. Bioanal. Chem.* **2011**, *400*, 709–714. [[CrossRef](#)] [[PubMed](#)]
38. González, M.G.; Domínguez-Renedo, O.; Alonso-Lomillo, M.A.; Martínez, M.A. Determination of gallium by adsorptive stripping voltammetry. *Talanta* **2004**, *62*, 457–462. [[CrossRef](#)]
39. Grabarczyk, M.; Wasag, J. Determination of trace amounts of Ga(III) by adsorptive stripping voltammetry with in situ plated bismuth film electrode. *Talanta* **2015**, *144*, 1091–1095. [[CrossRef](#)]
40. Kamat, J.; Guin, S.K.; Pillai, J.S.; Aggarwal, S.K. Scope of detection and determination of gallium(III) in industrial ground water by square wave anodic stripping voltammetry on bismuth film electrode. *Talanta* **2011**, *86*, 256–265. [[CrossRef](#)]
41. Medvecky, L.; Briancin, J. Possibilities of simultaneous determination of indium and gallium in binary InGa alloys by anodic stripping voltammetry in acetate buffer. *Chem. Pap.-Chem. Zvesti* **2004**, *58*, 93–100.
42. Pysarevska, S.; Dubenska, L. The advances in electrochemical determination of gallium (III). *Chem. Met. Alloy* **2018**, *11*, 34–41. [[CrossRef](#)]
43. Zhang, L.; Guo, X.; Li, H.; Yuan, Z.; Liu, X.; Xu, T. Separation of trace amounts of Ga and Ge in aqueous solution using nano-particles micro-column. *Talanta* **2011**, *85*, 2463–2469. [[CrossRef](#)] [[PubMed](#)]
44. Divrikli, U.; Soylak, M.; Elci, L. Separation and Enrichment of Gallium(III) as 4-(2-Thiazolylazo) Resorcinol (TAR) Complex by Solid Phase Extraction on Amberlite XAD-4 Adsorption Resin. *Anal. Lett.* **2003**, *36*, 839–852. [[CrossRef](#)]
45. Bermejo-Barrera, P.; Martínez-Alfonso, N.; Bermejo-Barrera, A. Separation of gallium and indium from ores matrix by sorption on Amberlite XAD-2 coated with PAN. *Anal. Bioanal. Chem.* **2001**, *369*, 191–194. [[CrossRef](#)]
46. Hassanien, M.M.; Kenawy, I.M.; El-Menshawy, A.M.; El-Asmy, A.A. Separation and Preconcentration of Gallium(III), Indium(III), and Thallium(III) Using New Hydrazone-modified Resin. *Anal. Sci.* **2008**, *23*, 1403–1408. [[CrossRef](#)] [[PubMed](#)]
47. Hassanien, M.M.; Kenawy, I.M.; Mostafa, M.R.; El-Dellay, H. Extraction of gallium, indium and thallium from aquatic media using amino silica gel modified by gallic acid. *Microchim. Acta* **2010**, *172*, 137–145. [[CrossRef](#)]
48. Nayak, S.; Devi, N. Studies on extraction of gallium (III) from chloride solution using Cyphos IL 104 and its removal from photodiodes and red mud. *Hydrometallurgy* **2017**, *171*, 191–197. [[CrossRef](#)]
49. Burylin, M.; Kopeyko, E.; Bokiy, E.; Konshin, V.; Konshina, D. Determination of indium in water samples using solid-phase extraction with modified silica gel and slurry sampling with electrothermal atomic absorption spectrometry. *Chem. Pap.* **2022**, *76*, 5893–5899. [[CrossRef](#)]
50. Furukawa, M.; Tateishi, I.; Katsumata, H.; Kaneko, S. Preconcentration of trace indium in aqueous samples using sodium dodecyl sulphate/activated carbon prior to electrothermal furnace absorption spectrometry. *Int. J. Environ. Anal. Chem.* **2019**, *101*, 719–733. [[CrossRef](#)]
51. Igosheva, V.S.; Zaitceva, P.V.; Vasil’Eva, N.L. Electrothermal atomic absorption indium determination. *AIP Conf. Proc.* **2019**, *2174*, 020022. [[CrossRef](#)]
52. Martínez, N.; Barrera, A.B.; Bermejo, B.P. Indium determination in different environmental materials by electrothermal atomic absorption spectrometry with Amberlite XAD-2 coated with 1-(2-pyridylazo)-2-naphthol. *Talanta* **2005**, *66*, 646–652. [[CrossRef](#)]
53. Minamisawa, H.; Murashima, K.; Minamisawa, M.; Arai, N.; Okutani, T. Determination of Indium by Graphite Furnace Atomic Absorption Spectrometry after Coprecipitation with Chitosan. *Anal. Sci.* **2003**, *19*, 401–404. [[CrossRef](#)] [[PubMed](#)]
54. Tuzen, M.; Soylak, M. A solid phase extraction procedure for Indium prior to its graphite furnace atomic absorption spectrometric determination. *J. Hazard. Mater.* **2006**, *129*, 179–185. [[CrossRef](#)]
55. Bernal, J.L.; Nozal, M.J.; Deban, L.; Aller, A.J. Determination of indium in aluminium alloys by flame atomic-absorption spectroscopy and flame atomic-emission spectrometry. *Talanta* **1982**, *29*, 1113–1116. [[CrossRef](#)] [[PubMed](#)]
56. Çelik, B.; Akkaya, E.; Bakirdere, S.; Aydin, F. Determination of indium using vortex assisted solid phase microextraction based on oleic acid coated magnetic nanoparticles combined with slotted quartz tube-flame atomic absorption spectrometry. *Microchem. J.* **2018**, *141*, 7–11. [[CrossRef](#)]
57. Donati, G.L.; Kron, B.E.; Jones, B.T. Simultaneous determination of Cr, Ga, In and V in soil and water samples by tungsten coil atomic emission spectrometry. *Spectrochim. Acta Part B At. Spectrosc.* **2009**, *64*, 559–564. [[CrossRef](#)]
58. Levine, K.E.; Han, L.; Gwinn, W.M.; Morgan, D.L.; Ross, G.T.; Essader, A.S.; Fernando, R.A.; Haines, L.G.; Robinson, V.G. Development and Optimization of a Procedure for the Determination of Indium-Tin Oxide Particle Size and Concentration in Cellular Media. *Anal. Lett.* **2014**, *47*, 1614–1625. [[CrossRef](#)]
59. Yang, D.; Chang, X.; Liu, Y.; Wang, S. Synthesis and application of spherical macroporous epoxy-polyamide chelating resin for preconcentration and separation of trace Ga(III), In(III), Bi(III), V(V), Cr(III), and Ti(IV) from solution samples. *J. Appl. Polym. Sci.* **2005**, *97*, 2330–2334. [[CrossRef](#)]
60. Zolfonoun, E.; Yousefi, S.R. Exfoliated graphitic carbon nitride nanosheets for on-line vortex-assisted dispersive micro-solid phase extraction of indium prior to determination by ICP-OES. *Int. J. Environ. Anal. Chem.* **2020**, *102*, 4031–4041. [[CrossRef](#)]

61. Alibo, D.S.; Amakawa, H.; Nozaki, Y. Determination of indium in natural waters by flow injection inductively coupled plasma mass spectrometry. *J. Earth Syst. Sci.* **1998**, *107*, 359–366. [[CrossRef](#)]
62. Liao, X.; Hu, Z.; Luo, T.; Zhang, W.; Liu, Y.; Zong, K.; Zhou, L.; Zhang, J. Determination of major and trace elements in geological samples by laser ablation solution sampling-inductively coupled plasma mass spectrometry. *J. Anal. At. Spectrom.* **2019**, *34*, 1126–1134. [[CrossRef](#)]
63. Pitzke, K.; Timm, K.; Hebisch, R.; Brock, T.; Hartwig, A.; MAK Commission. Indium—Determination of indium and its compounds in workplace air using mass spectrometry with inductively coupled plasma (ICP-MS). *MAK Collect. Occup. Health Saf.* **2021**, *6*, Doc044. [[CrossRef](#)]
64. Ferreira, E.D.M.M.; Morelli, T.; Moreira, I.M.N.S.; De Carvalho, M.S. Studies on indium sorption from iodide medium by polyurethane foam. *J. Braz. Chem. Soc.* **2004**, *15*, 563–569. [[CrossRef](#)]
65. Kazemi, E.; Shokoufi, N.; Shemirani, F. Indium determination and preconcentration using fiber optic linear array detection spectrometry combined with dispersive liquid-liquid micro extraction. *J. Anal. Chem.* **2011**, *66*, 924–929. [[CrossRef](#)]
66. Poledniok, J. A Sensitive Spectrophotometric Method for Determination of Trace Quantities of Indium in Soil. *Water Air Soil Pollut.* **2007**, *186*, 343–349. [[CrossRef](#)]
67. Shadmehri, E.A.; Abadi, M.D.M.; Chamsaz, M. Sensitive analysis In(III) in various matrices by spectrophotometry after dispersive liquid-liquid microextraction based on solidification of floating organic drop. *Russ. J. Appl. Chem.* **2014**, *87*, 689–695. [[CrossRef](#)]
68. Zhang, L.; Wang, Y.; Guo, X.; Yuan, Z.; Zhao, Z. Separation and preconcentration of trace indium(III) from environmental samples with nanometer-size titanium dioxide. *Hydrometallurgy* **2009**, *95*, 92–95. [[CrossRef](#)]
69. Afshar, E.A.; Taher, M.A.; Fazelirad, H.; Naghizadeh, M. Application of dispersive liquid–liquid–solidified floating organic drop microextraction and ETAAS for the preconcentration and determination of indium. *Anal. Bioanal. Chem.* **2017**, *409*, 1837–1843. [[CrossRef](#)]
70. Cui, T.; Zhu, X.; Wu, L.; Tan, X. Ultrasonic assisted dispersive liquid-liquid microextraction combined with flame atomic absorption spectrometry for determination of trace gallium in vanadium titanium magnetite. *Microchem. J.* **2020**, *157*, 104993. [[CrossRef](#)]
71. Peng, G.; He, Q.; Zhou, G.; Li, Y.; Su, X.; Liu, M.; Fan, L. Determination of heavy metals in water samples using dual-cloud point extraction coupled with inductively coupled plasma mass spectrometry. *Anal. Methods* **2015**, *7*, 6732–6739. [[CrossRef](#)]
72. Krawczyk-Coda, M.; Stanisz, E. Low cost adsorbents in ultrasound-assisted dispersive micro solid-phase extraction for simultaneous determination of indium and nickel by high-resolution continuum source graphite furnace atomic absorption spectrometry in soils and sediments. *Anal. Methods* **2018**, *10*, 2681–2690. [[CrossRef](#)]
73. Hacht, B. Gallium(III) ion hydrolysis under physiological conditions. *Bull. Korean Chem. Soc.* **2008**, *29*, 372–376.
74. Baes, C.F.; Mesmer, R.E. *The Hydrolysis of Cations*; Robert, E., Ed.; Krieger: Malabar, FL, USA, 1986.
75. Brom, M.; Franssen, G.M.; Joosten, L.; Gotthardt, M.; Boerman, O.C. The effect of purification of Ga-68-labeled exendin on in vivo distribution. *EJNMMI Res.* **2016**, *6*, 65. [[CrossRef](#)] [[PubMed](#)]
76. Bahri, Z.; Rezai, B.; Kowsari, E. Selective separation of gallium from zinc using flotation: Effect of solution pH value and the separation mechanism. *Miner. Eng.* **2016**, *86*, 104–113. [[CrossRef](#)]
77. Debnath, A.; Majumder, M.; Pal, M.; Das, N.S.; Chattopadhyay, K.K.; Saha, B. Enhanced Adsorption of Hexavalent Chromium onto Magnetic Calcium Ferrite Nanoparticles: Kinetic, Isotherm, and Neural Network Modeling. *J. Dispers. Sci. Technol.* **2016**, *37*, 1806–1818. [[CrossRef](#)]
78. Agrawal, S.; Singh, N.B. Removal of arsenic from aqueous solution by an adsorbent nickel ferrite-polyaniline nanocomposite. *Indian J. Chem. Technol.* **2016**, *23*, 374–383.
79. López-García, I.; Rivas, R.E.; Hernández-Córdoba, M. Use of sodium tungstate as a permanent chemical modifier for slurry sampling electrothermal atomic absorption spectrometric determination of indium in soils. *Anal. Bioanal. Chem.* **2008**, *391*, 1469–1474. [[CrossRef](#)]
80. Hassanien, M.M.; Mortada, W.I.; Kenawy, I.M.; El-Daly, H. Solid Phase Extraction and Preconcentration of Trace Gallium, Indium, and Thallium Using New Modified Amino Silica. *Appl. Spectrosc.* **2016**, *71*, 288–299. [[CrossRef](#)]
81. Liu, H.-M.; Jiang, J.-K.; Lin, Y.-H. Simultaneous Determination of Gallium(III) and Indium(III) in Urine and Water Samples with Cloud Point Extraction and by Inductively Coupled Plasma Optical Emission Spectrometry. *Anal. Lett.* **2012**, *45*, 2096–2107. [[CrossRef](#)]
82. Sitko, R.; Kocot, K.; Zawisza, B.; Feist, B.; Pytlakowska, K. Liquid-phase microextraction as an attractive tool for multielement trace analysis in combination with X-ray fluorescence spectrometry: An example of simultaneous determination of Fe, Co, Zn, Ga, Se and Pb in water samples. *J. Anal. At. Spectrom.* **2011**, *26*, 1979–1985. [[CrossRef](#)]
83. López-García, I.; Vicente-Martínez, Y.; Hernández-Córdoba, M. Determination of ultratraces of mercury species using separation with magnetic core-modified silver nanoparticles and electrothermal atomic absorption spectrometry. *J. Anal. At. Spectrom.* **2015**, *30*, 1980–1987. [[CrossRef](#)]
84. Silveira, A.; Fuchs, M.; Pinheiro, D.; Tanabe, E.; Bertuol, D. Recovery of indium from LCD screens of discarded cell phones. *Waste Manag.* **2015**, *45*, 334–342. [[CrossRef](#)] [[PubMed](#)]

85. Chung, Y.-F.; Tien, K.-W. Recovery of Gallium and Indium from Waste Light Emitting Diodes. *J. Korean Inst. Resour. Recycl.* **2020**, *29*, 81–88. [[CrossRef](#)]
86. Wood, S.A.; Samson, I.M. The aqueous geochemistry of gallium, germanium, indium and scandium. *Ore Geol. Rev.* **2006**, *28*, 57–102. [[CrossRef](#)]

Disclaimer/Publisher's Note: The statements, opinions and data contained in all publications are solely those of the individual author(s) and contributor(s) and not of MDPI and/or the editor(s). MDPI and/or the editor(s) disclaim responsibility for any injury to people or property resulting from any ideas, methods, instructions or products referred to in the content.